MEDDOCS
Open Access Publisher

ISSN: 2690-8662

Journal of Clinical Images

Open Access | Research Article

Suitability of Different mAs-Reduced Ultra-Low-Dose CBCT Protocols for Peridental Bone Assessment Iin Pediatric Orthodontic Imaging

***Pinar Eric*[1]*; Hamza Zukorlic*[2]*; Axel Bumann*[1,2]**

[1]*MESANTIS Berlin, 3D DENTAL Radiologicum, Georgenstr. 25, 10117 Berlin, Germany.*

[2]*A+ Orthodontists Berlin, Georgenstr. 25, 10117 Berlin, Germany.*

***Corresponding Author(s): Pinar Eric**

MESANTIS Berlin, 3D DENTAL Radiologicum, Georgenstr. 25, 10117 Berlin, Germany.

Email: pinar.eric.zm@gmail.com

Received: Nov 01, 2023

Accepted: Nov 22, 2023

Published Online: Nov 29, 2023

Journal: Journal of Clinical Images

Publisher: MedDocs Publishers LLC

Online edition: http://meddocsonline.org/

Abstract

Background: Since decades panoramic x-rays and lateral cephalograms are Conventional Orthodontic Radiographs (COR). Lately, cone beam CT (CBCT) is becoming increasingly popular, but is still highly debated due to its higher radiation exposure when compared to COR. The development of so-called mAs-reduced CBCT protocols or Ultra-Low-Dose (ULD) protocols allows for significant lower radiation exposure. However, there are still ongoing discussions whether those protocols provide a sufficient image quality for orthodontic treatment planning of delicate peridental bone structures.

Objective: The purpose of this study was to evaluate the accuracy of detecting oral and vestibular bony dehiscences, using two different new mAs-reduced CBCT protocols with a further reduced effective dose.

Material and methods: Bony dehiscences of 14 human macerated skulls with 318 teeth and 636 dehiscences (oral and vestibular) were studied. Two CBCT protocols (protocol A: 20x17 cm, 200µm, 90 kV, 85.2 mAs, 58 µSv and protocol B: 20x17 cm, 200µm, 90 kV, 38.4 mAs, 26 µSv) were obtained from the skulls using the ProMax 3D Mid (Planmeca, Helsinki, Finland). An intraoral scan with Trios 3 (3 Shape, Copenhagen, Denmark) served as gold standard. Bony dehiscences were measured in the NemoStudio software (Nemotec, Leganes, Spain) in both protocols and compared with the values from the intraoral scans. Measurements were statistically analyzed using the t-test, single-factor analysis of variance, and Pearson's correlation coefficient in SPSS Statistics (version 27, IBM). Correlations to the gold standard were visualized in Bland-Altman plots.

Results: Intrarater reliability showed no significant differences for the gold standard for vestibular or oral, protocol A and B, respectively (protocol A: p= .998, p= .991; protocol B: p=.998, p=.994).

Cite this article: Rajagopalan R. An Interesting Case of Chromonychia in an Immunosuppressed Individual. J Clin Images. 2023; 6(2): 1151.

The measurements of the experimental protocols (A and B) did not deviate significantly from the gold standard. This was also confirmed by Pearson's correlation coefficient (A: R=0.960 and 0.985; B: R=0.952 and 0.981).

In addition, there was no significant difference between the two mAs-reduced protocols, neither forvestibular dehiscences (p=0.509) nor for oral dehiscences (p=0.515).

Conclusion: The results of the present study demonstrated that bony dehiscences can be reliably detected with mAs-reduced CBCT protocols at 200 µm resolution. Because of the low radiation dose the investigated mAs-reduced protocols allow the use of CBCT for pediatric orthodontic imaging. Regarding the detection of bony dehiscences prior to orthodontic tooth movement, these results are of great importance for pediatric orthodontic treatment planning.

Introduction

Most orthodontic patients have crowding [1]. Therefore, the primary goal is often to expand the alveolar arch [2]. To eliminate crowding and create space, the teeth must be moved vestibularly.

Adverse side effects of orthodontic treatment include mucosal defects and bone lesions. In addition, the literature shows a relationship between alveolar bone resorption and orthodontic therapy [3,4]. However, bony dehiscences and fenestrations also occur in the untreated dentition [5]. Therefore, it is essential to adequately assess the bony conditions of the jaw before treatment. Accordingly, the survey of the peridental bone supply is an important pretherapeutic measure [3,6]. Alveolar bone morphology is a limiting factor for orthodontic treatment, making analysis of peridental bone before orthodontic treatment inevitable [5,7].

Bone defects are increasingly identified through two-dimensional imaging techniques. The fact that information from a three-dimensional space is compressed into a two-dimensional image may result in distorted information [8]. Information may be lost on a panoramic radiograph because it is "superimposed" and thus cannot be faithfully represented [8,9]. Compared with conventional imaging techniques, CBCT has the great advantage that many more bony defects can be detected and measured [10,11,12].

Since the bone morphology can be depicted faithfully in CBCT images, the maximum tooth movement during therapy is easier for the practitioner to recognize. CBCT diagnosis in orthodontics helps the practitioner to develop an individualized treatment plan for the patient [4,6,7,13]. Although three-dimensional imaging can depict bony structures more faithfully than two-dimensional imaging, CBCT is not necessarily used pretherapeutically in daily practice due to the higher radiation exposure.

CBCT standard protocols have a very high effective dose of 220 µSv. Over the last five years, there has been an increase in study protocols that show a significant reduction in effective doses by reducing mAs values. The reduction of mAs values results in a linear reduction in effective radiation [6,14,15,16,17]. In the literature, a reduction of the effective dose by up to -79% can be found [16]. These values place 20-40 µSv effective dose per cone beam exposure in the range of two-dimensional radiographs.

Some authors recommend different radiation protection concepts, such as ALARA (As Low As Reasonably Achievable) [18,19] to ALADA (As Low As Diagnostically Acceptable) [20,21]. The difference here is that in the ALADA concept, the radiation dose is kept to a maximum of what is diagnostically necessary. A razor-sharp image is not necessary; only the diagnostically relevant part must be adequately displayed.

In addition to reducing the effective dose, diagnostically sufficient image quality is also of great importance. Some studies have addressed whether the reduction of mA values is accompanied by a deterioration of image quality and whether the image is then still diagnostically sufficient [6,23]. A sound knowledge of the change in effective dose as a function of image quality plays an important role in the implementation of the latest concept ALADA-iP (acceptable, indication-based, and patient-specific) [11].

With this concept and the adjustment of the appropriate parameters, it is possible to produce diagnostic-quality CBCT images while significantly reducing the radiation dose. However, a reduction in mAs values may lead to a degradation of image quality. Therefore, it needs to be clarified whether this deterioration in image quality has a negative impact on diagnosis or whether the images still have sufficient diagnostic value. In some studies, a reduction to 4 mA was performed, which still resulted in a diagnostically adequate image. Reducing mA values to 4 mA did not show a significant impact on image quality [6,23].

A recent meta-review examined publications addressing the radiation dose of CBCT images in dentistry [24]. The meta-review calls for further studies on effective dose directly related to image quality. Therefore, the present study follows this call and investigates the direct relationship between mAs reduction and image quality. The aim is to be able to perform optimal bone measurements in a CBCT while achieving an immense reduction in effective radiation.

Figure 1: Objects for examination; human, macerated skulls.

Material and Methods

In the present study, the CBCT images of 14 macerated human skulls were examined. For this purpose, 318 teeth with 636 dehiscences (oral and vestibular) were included in the study. Two CBCT images were acquired from each skull using the ProMax 3D Mid CBCT unit (Planmeca, Helsinki, Finland). Images were acquired using two different protocols, resulting in a total of 28 data sets examined (protocol A: field of view (FoV) 20 x 17 cm, voxel size 200 µm, current voltage 90 kV, exposure time 12 s, current intensity 6.0 mA, current intensity per second 72 mAs; protocol B: field of view (FoV) 20 x 17 cm, voxel size 200 µm, current

voltage 90 kV, exposure time 12 s, current intensity 3.2 mA, current intensity per second 38.4 mAs). Both protocols are reduced in their mAs values compared to standard protocols, whereas protocol B shows a stronger mAs reduction than protocol A.

The skulls were additionally scanned with the Trios 3 intraoral scanner (Shape, Copenhagen, Denmark, see **Table 1**). The digitally generated three-dimensional image matched the original object very well due to the precise scanning and is therefore considered the gold standard in the present work.

Subsequently, the scans were imported into Nemotec software (Nemo Studio 2019, Nemotec, Madrid, Spain) with the CBCT NemStudio datasets and measured. NemoStudio is a dental software used in wide areas of dentistry, such as implantology and orthodontics. In the software, it is possible to merge three-dimensional radiographs (such as CBCT with STL datasets) by superimposition (matching). In the present work, this aspect was of great importance. The measurement points on the X-ray image as well as in the STL file from the intraoral scan (gold standard) were thus at the same position. Thus, measurement inaccuracies could be reduced.

The DICOM and STL data sets were uploaded individually to the Nemo Studio software. In the software, the teeth were aligned and overlaid (matched) in all three spatial planes. After matching, the vestibular and oral bone dehiscences were measured individually.

First, the height of the enamel-cement interface was marked in the DICOM dataset. This mark was also seen in the STL dataset at the height of the enamel-cement interface.

The distance between the enamel-cement interface and the upper margin of the crestal alveolar bone was measured as dehiscence. The measurement was performed on both the vestibular and oral sides in both the STL and DICOM data sets.

For each protocol, four measurement series per dehiscence were measured by one rater. A total of 5088 measurements were available.

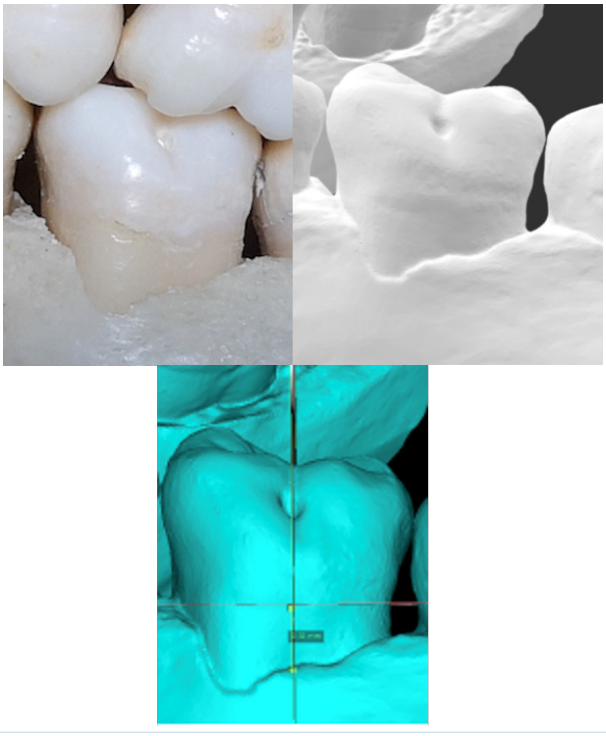

Figure 2: Photo of a molar, intraoral scan of a molar, match of CBCT and intraoral scan of a molar.

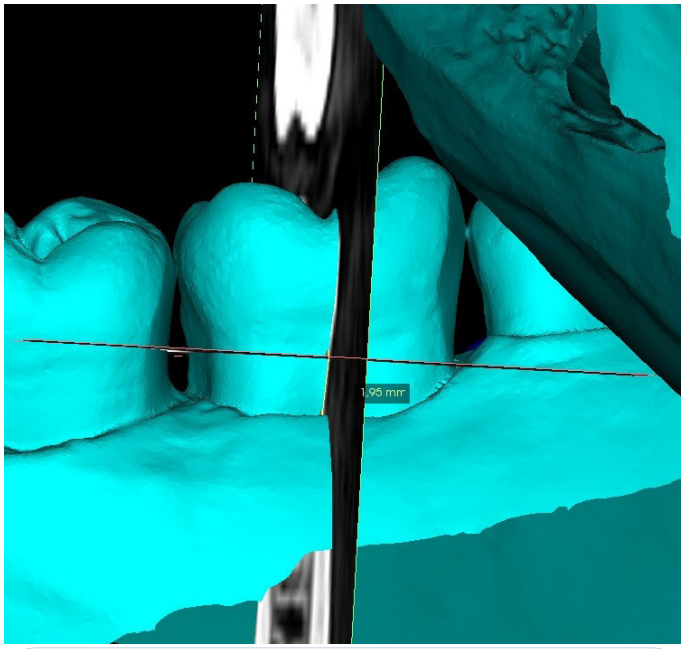

Figure 3: Nemo Studio, oral view of molar dehiscences of a molar.

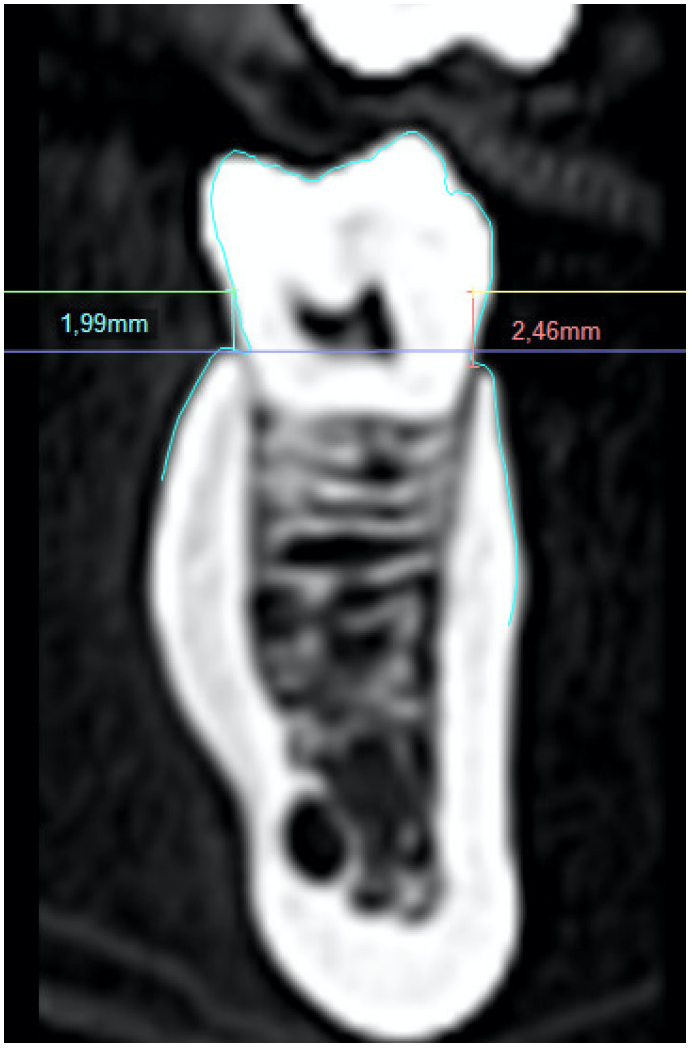

Figure 4: Measurement of oraland vestibular.

A single-factor analysis of variance was performed, and the measurement time points were compared to statistically determine reproducibility. The Intraoral Scanner (STL) measurements represent the gold standard in this work. A correlation analysis was performed in person to determine the correlation between

the measurements from the DICOM datasets for protocols A and B with the measurements from the STL datasets. A paired-samples t-test was also performed for direct comparison of the two protocols, and Bland-Altman plots were generated. Data was collected in Excel spreadsheets and transferred to IBM SPSS Statistics for statistical analysis.

Results

Reproducibility of bone dehiscences in intraoral scan, protocols A and B

Intraoral scan

The reliability of the intraoral scan showed no statistically significant differences in its four measurement series, neither for oral, nor for vestibular. Single factor analysis of variance was performed to compare the four measurement time points. According to the f-statistic, the values of the four measurement series have not statistically significantly different from each other (F (3.1206) = .013; p = .998; F (3.1206) = .034; p = .991).

Figure 5 shows the differences in the measured values of the dehiscences of the intraoral scanner together with their frequencies. A normal distribution with a rightward shift can be seen. Here, the absolute mean difference is present as a maximum value at 0.10 mm.

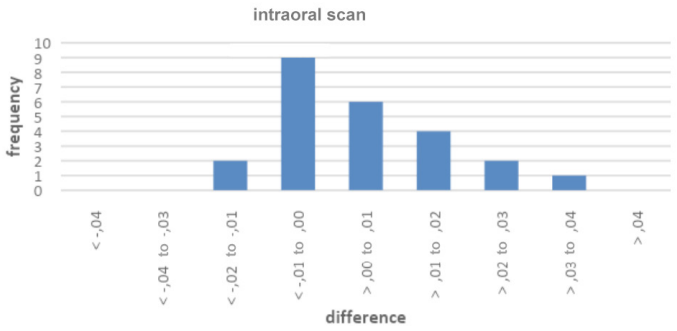

Figure 5: "Intraoral scan": The reliability of the four measurement series shown in a bar chart with the differences in mm.

Table 1: Summary of the absolute mean difference and its upper and lower limits (95% confidence interval). Intraoral scan of the dehiscences measured in mm.

	Mean difference	lowerlimit	upperlimit	SD
STL vestibular	0.008	-0.005	0.017	1.49
STL vest./oral	0.002	-0.012	0.014	1.26
STL oral	0.010	-0.013	0.033	1.25
STL vest/oral	-0.003	-0.010	0.006	1.24

Protocol A

The reliability of the measurements of protocol A showed no statistically significant differences in its four measurement series, neither for oral, nor for vestibular. Single factor analysis of variance was performed to compare the four measurement time points Single factor analysis of variance was performed to compare the four measurement time points. According to the f statistic, the values of the four measurement series have no statistically significant difference (F (3.1207) = .017; p = .997; F (3.1207) = .040; p = .989).

Figure 6 represents the deviations in the measured values of the dehiscences for Protocol A, together with its frequencies. For the diagram of the reliability of Protocol A, a slight shift to the right of up to 0.2 - 0.3 mm can be seen. Most of the deviations are in the range of -0.1 mm to 0.1 mm. The largest mean deviation is 0.016 mm (**Table 5**).

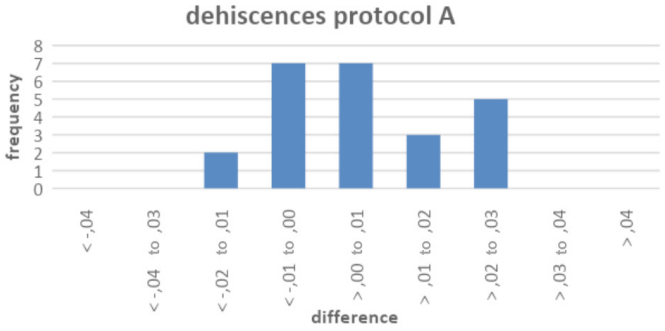

Figure 6: "Protocol A": The reliability of the four measurement series shown in a bar chart with the differences in mm.

Table 2: Summary table of the absolute mean difference, with its upper and lower limits (95% confidence interval) of the dehiscences for Protocol A in mm.

	Mean difference	lower limit	upper limit	SD
dehiscence vestibular	0.016	-0.001	0.023	1.60
dehiscence vestibular distal	0.000	-0.010	0.005	1.25
dehiscence oral	0.014	-0.002	0.025	1.30
dehiscence oral distal	0.003	-0.012	0.013	1.56

Protocol B

The reliability of the measurements of protocol A showed no statistically significant differences in its four measurement series, neither for oral, nor for vestibular. Single factor analysis of variance was performed to compare the four measurement time points. The values of the four measurement series have no statistically significant difference (F (3.1183) = .009; p = .999; F (3.1183) = .003; p = 1.000). For the measured values of the dehiscences of Protocol B, the Mean (M), Standard Deviation (SD) and mean difference were also determined using statistical calculations (**Table 7**). **Figure 7** presents the deviations of the measured values of the dehiscences for Protocol B, together with its frequencies. A shift in the positive direction can be seen with respect to the bar chart of the reliability for Protocol B (**Figure 4**). In the negative range there are deviations from -0.1 mm to 0 mm, and in the positive range the deviations extend up to 0.4 mm. The largest mean deviation is 0.027 mm (**Table 7**).

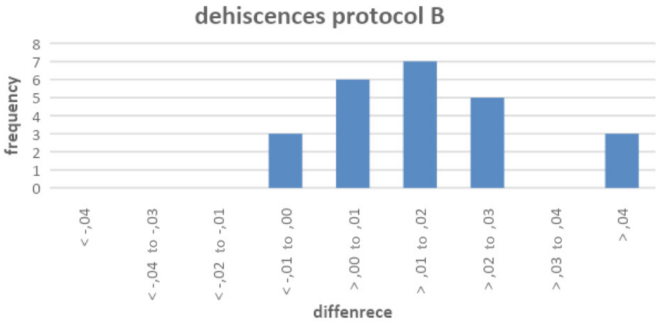

Figure 7: "Protocol B": The reliability of the four measurement series, shown in a bar chart with the differences for bone thickness measured in mm.

Table 3: Summary of the absolute mean difference and its upper and lower limits (confidence interval 95 %). Dehiscencesfor Protocol Bshown in mm.

	Mean difference	Lower limit	Upper limit	SD
dehiscence vestibular	0.013	0.001	0.022	1.64
dehiscence vestibular distal	0.007	-0.005	0.017	1.28
dehiscence oral	0.013	0.001	0.024	1.32
Dehiscenceoral distal	0.027	-0.002	0.050	1.56

Deviation of bone measurements of both protocols from the gold standard

Protocol A

There is no statistic significant difference between the vestibular measurements from the CBCT dataset for Protocol A and the measurements from the Intraoral Scan (STL). Pearson's correlation coefficient is 0.960 for the vestibular measurements, representing a very high correlation. A t-test confirmed this strong correlation ($P < 0.01$). The values of the vestibular dehiscences of the DICOM dataset for protocol A were plotted, along with the respective values of the STL dataset, in a Bland-Altman plot. The mean of both measurements was plotted on the x-axis, and the difference of both measurements was plotted on the y-axis. The LoA (Limits of Agreement) are defined as +1.0 mm for the upper limit and -0.81 mm for the lower limit. Within these limits, 95% of the differences and mean values of the measurements are located. **Figure 8** shows a very high density of values on the straight line of the mean difference. This means that most of the values have very small to no measurement differences. Most of the values are very close together to, just below, on, or above the straight line mean difference.

A few of the values are well outside the mean difference, and represent outlier values at 1%. The mean absolute difference between the DICOM protocol A and STL measurements is 0.09 mm for the vestibular measurements, well below the clinical tolerance range.

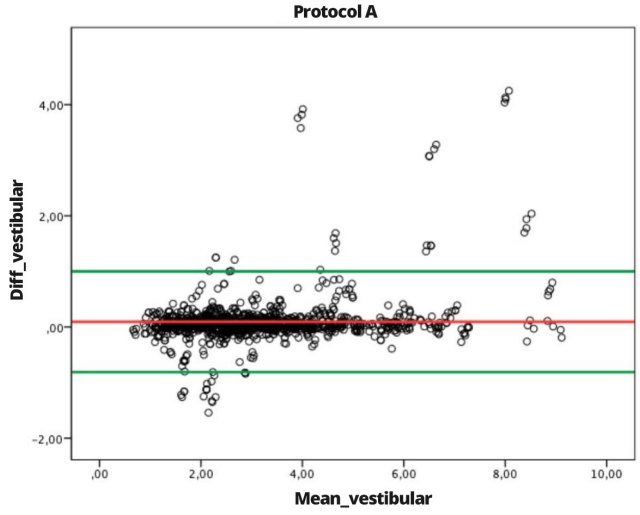

Figure 8: This Bland-Altman plot shows the correlation between the two series of measurements for the vestibular dehiscences of Protocol A for the DICOM and STL datasets. The red line shows the mean difference as a straight line (bias), the green lines are the limits of agreement (LoA 95% confidence interval).

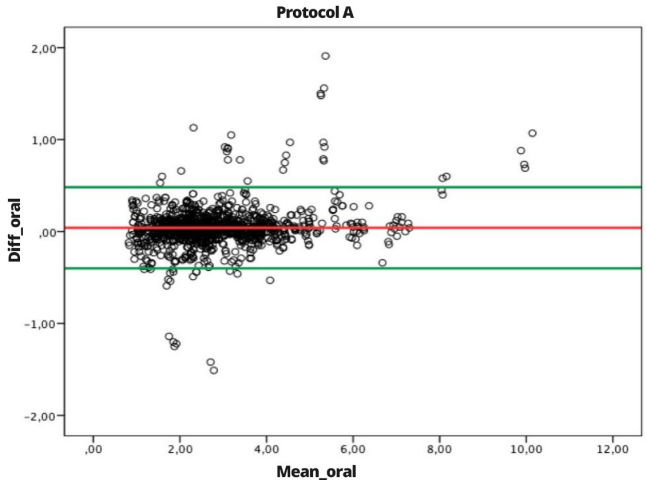

Figure 9: This Bland-Altman plot shows the correlation between the two series of measurements for the oral dehiscences of Protocol A of the DICOM and STL datasets. The red line shows the mean difference as a straight line (bias), the green lines are the limits of agreement (LoA 95% confidence interval).

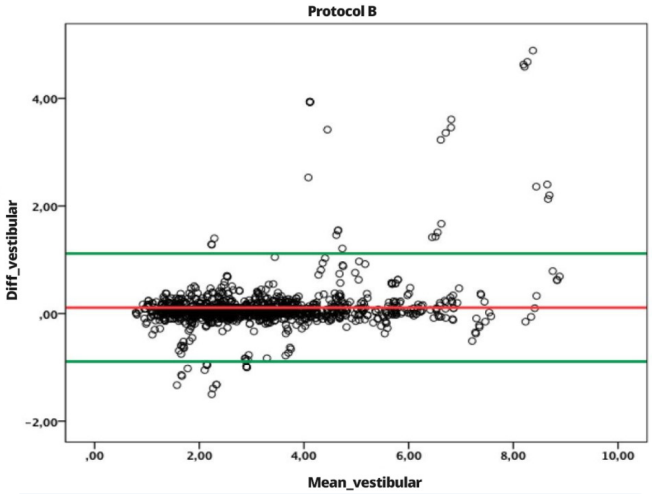

Figure 10: This Bland-Altman plot shows the correlation between the two series of measurements for the vestibular dehiscences of Protocol B of the DICOM and STL datasets. The red line shows the mean difference as a straight line (bias), the green lines are the limits of agreement (LoA 95% confidence interval).

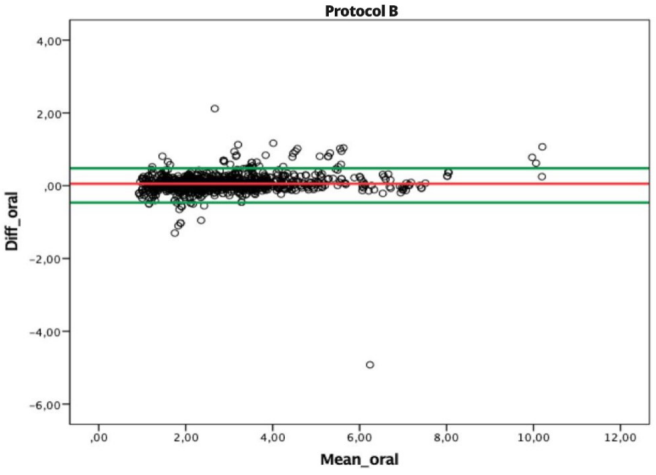

Figure 11: This Bland-Altman plot shows the correlation between the two series of measurements for the oral dehiscences of Protocol B of the DICOM and STL datasets. The red line shows the mean difference as a straight line (bias), the green lines are the limits of agreement (LoA 95% confidence interval).

Protocol B

There is no significant difference between the oral measurements from the CBCT data set for Protocol B and the measurements from the Intraoral Scan (STL). The Pearson correlation coefficient for the oral measurements is 0.981, representing a very strong correlation. A t-test confirmed this strong correlation ($p > 0.001$).

The values of the oral dehiscences of the DICOM dataset for Protocol B were plotted with the respective values of the STL dataset in a Bland-Altman diagram. The mean of both measurements was plotted on the x-axis and the difference between both measurements was plotted on the y-axis. The LoA (Limits of Agreement) are defined as +0.57 mm for the upper limit and -0.46 mm for the lower limit. Within these limits, 95% of the differences and mean values of the measurements are located. **Figure 10** shows a very high density of values on the straight line of the mean difference. This means that most of the values have very small to no measurement differences. Most of the values are very close together. A few values are far outside the mean difference, and represent outlier values of 0.2%.

The mean absolute difference between the DICOM protocol B and STL measurements is 0.05 mm for the oral measurements, well below the clinical tolerance range.

Deviation of bone measurements between protocols A and B

The determined vestibular dehiscences in mm are almost identical in protocols A and B. There are no significant differences between the measurements of vestibular dehiscences for both protocols (p-value = 0.509). The mean values of the vestibular dehiscences of both protocols are therefore very close to each other, and show a very high level of agreement. **Figure 12** shows the mean values of the vestibular dehiscences of protocols A and B in a bar chart. The mean value of the vestibular dehiscences for Protocol A is 3.24 mm. The mean value of vestibular dehiscences for Protocol B is 3.27 mm. There is a difference of 0.03 mm in the mean values for both protocols.

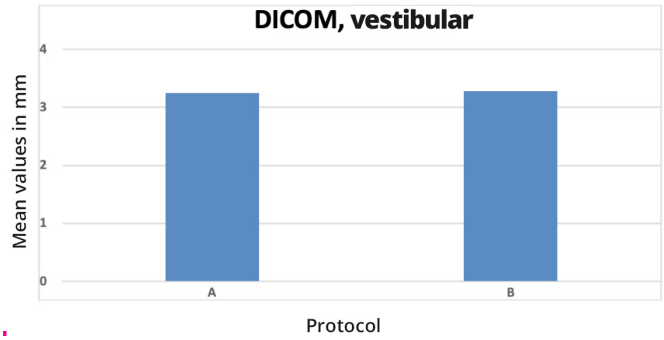

Figure 12: Mean values of the vestibular dehiscences of protocols A and B in mm.

The determined oral dehiscences in mm are almost identical in protocols A and B. There are no significant differences between the measurements of oral dehiscences for both protocols (p-value = 0.515). Chart 11 presents the mean values of oral dehiscences for protocols A and B in a bar graph. The mean value of oral dehiscences for Protocol A is 2.84 mm. The mean value of oral dehiscences for Protocol B is 2.88 mm. There is a difference of 0.04 mm in the mean values for both protocols. There is a small difference of 0.04 mm in the mean values of protocols A and B. The mean values for the oral dehiscences of both protocols are therefore very close to each other, showing a very high level of agreement.

Table 4: Mean differences, upper and lower limits, p-values of vestibular, vestibular-distal, oral and oral-distal dehiscences for protocols A and B.

	Protocol A			Protocol B			Mean difference
	mD	uG	oG	mD	uG	oG	p-Wert
DICOM, vestibulär	0,016	-0,001	0,023	0,013	0,001	0,022	0,509
DICOM, vest./dist	0,000	-0,010	0,005	0,007	-0,005	0,017	0,547
ICOM, oral	0,014	-0,002	0,025	0,013	0,001	0,024	0,515
DICOM, oral/dist	0,003	-0,012	0,013	0,027	-0,002	0,050	0,411

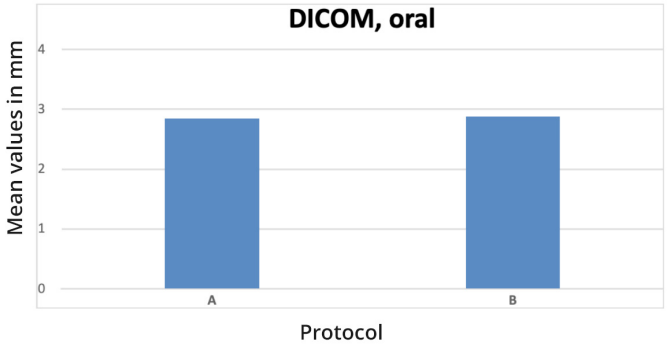

Figure 13: Mean values of the oral dehiscences of protocols A and B in mm.

Discussion

Due to the high prevalence of bone defects, bone measurements should be taken by X-ray prior to orthodontic treatment in order to establish an adequate treatment plan. CBCT has the advantage of showing dehiscences in oral and vestibular directions more naturally. Since most patients in orthodontics are children and adolescents, the issue of reducing the effective dose is particularly important here.

There are currently over 85 different CBCT devices on the market, all with different features and functions [10]. In particular, it is difficult to evaluate the effective doses between them because the parameters are set differently. Various analyses have shown that the effective dose of different CBCT devices ranges from 5 µSv to 1073 µSv [25, 26,27].

These studies show the wide range of effective doses of the various CBCT devices on the market. According to them, the different doses depend on the device, the FoV, and the setting parameters such as current voltage, tube intensity, and exposure time [52]. This range is highly unsuitable for clinical use. Various investigators have attempted to reduce the radiation dose by changing the parameters and using different protocols. Studies have been performed in which the Fov, current voltage kV, voxel size, or exposure time were changed [10,27,28,29,30]. In the

studies, some investigators note a reduction in radiation exposure, but this is often accompanied by a degradation in image quality. The change in image quality due to noise or a decrease in image contrast represents the limits of altered parameters.

In our study, the radiation dose with the manufacturer's recommended protocols is 263 µSv at 360 mAs. The effective dose with the manufacturer's lower protocols is 117.2 mAs at 83 µSv. For comparison, a panoramic slice exposure is approximately 20 µSv.

The optimal CBCT protocol is the one that has the lowest possible radiation exposure without compromising diagnostic value through image quality degradation. In our case, this means reducing the mAs enough to keep the radiation exposure at the level of a standard panoramic radiograph.

The purpose of this study is to compare the radiographs to the gold standard and determine if further reduction of mAs has an impact on the accuracy of diagnosis of peridental bone.

As also our present study Several studies have investigated how to modify the parameters of CBCT protocols to achieve a reduction in radiation dose while maintaining the same image quality or adequate diagnostic accuracy. Some of these studies have shown that image quality was adequate for the diagnosis of bone defects when mAs were reduced to a maximum of 4 mA. Similar to the present study no significant differences were found between the different protocols.

Sur et al. 2010 investigated the reduction of mAs from 6 mAs to 2 mAs in macerated skulls. Ten investigators compared the results and concluded that the reduction in mAs had no effect on diagnostic image quality for objective bone measurements. There was sufficient agreement for qualitative assessment of CBCT images.

Tangari-Meira et al. (2017) performed studies with different mA values between 4 and 10 mA and found no significant differences in image quality. In 2018, Panmekiate et al. analyzed the optimal balance between parameters of CBCT images. They found that reducing the mA value by up to 40% is possible to reduce the radiation dose while maintaining adequate image quality.

A significant reduction in effective dose can be achieved by decreasing the mAs value without significantly decreasing image quality when assessing bone ratio [6]. The present work follows up on these findings by evaluating two different mA-reduced protocols for their accuracy in diagnosing bone defects. The results of this work show that the diagnostic value even for the mA-reduced protocol (3.2 mA) for linear bone measurements with the previously mentioned parameters has no significant difference compared to CBCT images with higher mA values.

Thus, the results of our study are consistent with those cited in the finding that reducing mAs down to 4 mA does not significantly degrade image quality.

Furthermore, the reproducibility of the measurement method depends on the conditions of the measurement method. In the present work, measurements were performed according to a stan-dardized measurement methodology based on published studies by Fuhrmann (1996), Evangelista (2010), Lee (2012), Jäger (2015), and Elefant (2015). Here, the alignment of the respective teeth to be measured in all three spatial planes was a condition to ensure reproducibility.

With this precise alignment, it is possible to steadily place the teeth in the same position and measure them. Determining the enamel-cement interface in the STL file of the intraoral scan proved to be a challenge. The measurement of the lower anterior teeth was particularly critical due to the smooth transition from enamel to root dentin. Since the transition from enamel to root cementum was often difficult to determine in the scans on the lower anterior teeth, the scatter of mean deviations tended to be highest here compared to the other tooth groups. The single factor analysis of variance confirmed the reproducibility of the bone dehiscences in the present intraoral scan.

With regard to the high clinical prevalence and the low effective doses, evaluation of the peridental bone availability seems to be a main justified indication prior to orthodontic treatment planning. The introduced mAs-reduced ultra-low-dose protocols provide the same or even less effective dose when compared with the effective dose of COR. This means, the clinician has 3D treatment planning information with less dose than with traditional COR.

In the future, the clinical discussion shouldn´t be directed to the decision panoramic x-ray/lateral ceph or CBCT, but rather which specific CBCT protocol should be used for orthodontic treatment planning.

Table 5: Parameters of the mA reduced protocols A and B.

Protocol	Fov	µSv	kV	mA	Time	mAs	Effective Dose
A	20x17	200	90	6.0	12.0	72	54
B	20x17	200	90	3.2	12.0	38.4	29

Conclusion

MAs-reduced ultra-low-dose CBCT protocols with a resolution of 200 µm allow for a reliable quantification of peridental bone structures, especially bony dehiscences. These results are important for daily planning of orthodontic tooth movements and its limitations. With the investigated mAs-reduced ultra-low-dose CBCT protocols the effective dose can be - especially for children - significantly reduced to values lower than with 2D images.

References

1. J Clin Pediatr Dent. Gudipanemi Ravi Kumar, Alam Mohammad Khursheed, Patil R Santosh, Karobari Mohmed Isaqali. 2020; 44: 423-428.
2. D´Souza Ivor M, Kumar Kiran H C, Shetty Sadashiva Dental arch changes associated with rapid maxillary expansion: A retrospective model analysis study. Contemp Clin Dent. 2015; 6: 51-57.
3. Sun L, Yuan L, Wang B, Shen G, Fang B, et al. Changes of alveolar bone dehiscence and fenestration after augmented corticotomy-assisted orthodontic treatment: A CBCT evaluation. Prog Orthod. 2019; 20: 7
4. Filipova D, T Dostalova, V Filipi, M Kaminek. Proclination-induces changes in the labial cortical bone thickness of lower incisors. Bratisl Lek Listy. 2019; 120: 155-160
5. Gambarini, Miccoli, Gaimari, Pompei, Pilloni, Piasecki, et al. Detection of Bone Defects Using CBCT Exam in an Italian Population. Int J Dent. 2017.
6. Feragalli Beatrice, Osvaldo Rampado, Cecilia Abate, Monica Macri, Felice Festa, et al. Cone beam computed tomography for dental and maxillofacial imaging: technique improvement and low-dose protocols. Radio Med . 2017; 122: 581-588.

7. Coskun ipek, Burcak kaya. Appraisal of the relationship between tooth inclination, dehiscence, fenestration, and sagittal skeletal pattern with cone beam computed tomography. Angle Ortho 2019; 89: 544-551.

8. Machado GL. CBCT imaging - A boon to orthodontics. Saudi Dent J. 2015; 27: 12-21.

9. Küker NJ. Metrischer Vergleich von CT, DVT und konventionellen Röntgentechniken in der MKG-Chirurgie. Fakultät der Universität Hamburg. 2010.

10. Jacobs Reinhilde, Benjamin Salmon, Marina Codari, Bassam Hassan, Michael M Bornstein. Cone beam computes tomography in implant dentistry: Recommendations for clinical use. BMC Oral Health. 2018; 18: 88.

11. Oenning AC, Pauwels R, Stratis A, De Faria Vasconcelos K, Tijskens E, et al. Dimitra research group, Jacobs R, Salmon B. Halve the dose while maintaining image quality in pediatric Cone Beam CT. Free PMC article clinical trial. 2019; 9: 5521.

12. Abdinian Mehrdad, Jaber Yaghini, Leila Jazi. Comparison of intraoral digital radiography and cone-beam computed tomography in the measurement of periodontal bone defects. Dent Med Probl. 2020; 57: 269-273.

13. Akshaya Bhupesh Banoskar, Rajesh Prabhakar Gaikwad, Tanay Udayrao Gunjikar, Tanya Arthur Lobo. Evaluation of accuracy of cone beam computed tomography for measurement of periodontal defects: A clinical study. J Indian Soc Periodontol. 2015; 19: 285-289.

14. D Chambers, R Bohay, L Kaci, R Barnett, J Battista, et al. The effective dose of different scanning protocols using the Sirona GALILEOS(®) comfort CBCT scanner. Dentomaxillofac Radiol. 2015; 44: 20140287.

15. Währisch Kristin Anabelle. Vergleich der Strahlen-belastung von konventionellen orthodontischen Röntgen-aufnahmen mit konventionellen und indikationsabhängigen dosisreduzierten digitalen Volumentomographien. Universität Berlin. 2015.

16. Schwabl D. Evaluierung der Effektivdosis verschiedener zahnärztlich radiologischer Verfahren an der Medizinischen Universität Graz. Medizinische Universität Graz. 2018.

17. Voigt Susanne. Vergleichende Untersuchungen zur kephalometrischen Auswertbarkeit von konventionellen Fernröntgenseitenbildern und aus IADR-DVT-Datensätzen rekonstruierten Fernröntgenansichten. Universität Berlin. 2018.

18. Tandheelkd Ned Tijdschr. The ALARA-principle. Backgrounds and enforcement in dental practices. WER Berkhout. 2015; 122: 263-270.

19. Frane Nicholas, Bitterman Adam. Radiation Safety and Protection. Stat Pearls Publishing. 2021.

20. Kofler Barbara, Jenetten Laura, Runge Annette, Degenhart Gerald, Hörmann Romed, et al. ALADA Dose Optimization in the Computed Tomography of the Temporal Bone: The Diagnostic Potential of Different Low-Dose CT Protocols. Diagnostics Basel. 2021; 15: 1894.

21. Jaju P Prashant, Jaju P Sushma. Cone-beam computed tomography: Time to move from ALARA to ALADA. Imaging Sci Dent. 2015; 45: 263-265.

22. Panmekiate S, Peera Rungwittayathon, Wijuck Suptaweeponboon, Nattarus Tangtraiitham, Ruben Pauwels, et al. Optimization of exposure parameters in dental cone beam computed tomography using a 3-step approach. Oral Surg Oral Med Oral Pathol Oral Radiol. 2018; 126: 545-552.

23. Tangari-Meira Ricardo, Jose Ricardo Vancetto, Livia Nord Dovigo, Guilherme Monteiro Tosoni, et al. Influence of tube current settings on diagnostic detection of root fractures using cone-beam computed tomography. J Endod. 2017; 43: 1701-1705.

24. Al-Okshi A, Nilsson M, Petersson A, Wiese M, Lindh C, et al. Using Gaf Chromic film to estimate the effective dose from dental cone beam CT and panoramic radiography. Dento maxillo facial radiology. Dento maxillo facial radiology. 2013; 42: 20120343.

25. Rottke Dennis, Jonas Andersson , Ken-Ichiro Ejima , Kunihiki Sawada , Dirk Schulze, et al. Influence of lead apron shielding on absorbed doses from cone-beam computed tomography. Radiat Prot Dosimetry. 2017; 175: 110-117.

26. Ludlow JB, Timothy R, Walker C, Hunter R, Benavides E, et al. Effective dose of dental CBCT-a meta analysis of published data and additional data for nine CBCT units. Dento maxillo facial radiology. 2015; 44: 20140197.

27. R Pauwels, R Jacobs, SR Singer, M Mupparapu. CBCT-based bone quality assessment: are Hounsfield units applicable? Dentomaxillofac Radiol. 2015; 44: 20140238.

28. Lagos ML, Sant'ana AC, Greghi SL, Passanezi E. Keratinized Gingiva Determines a Homeostatic Behavior of Gingival Sulcus through Transudation of Gingival Crevice Fluid. International Journal of Dentistry. 2011.

29. Davies J, Johnson B, Drage N. Effective doses from cone beam CT investigation of the jaws. Dentomaxillofac Radiol. 2012; 41: 30–36.

30. Dach Eva, Bastian Bergauer, Anna Seid, Cornelius von Wilmowsky, Wermer Adler, et al. Impact of voxel size and scan time on the accuracy of three-dimensional radiological imaging data from cone-beam computed tomography. J Craniomaxillofac Surg. 2018; 46: 2190-2196.